Enhanced Simulation of Guided Waves and Damage Localization in Composite Strips Using the Multiresolution Finite Wavelet Domain Method

Dimitris Dimitriou[1(✉)] , Christos Nastos[1,2] ,
and Dimitris Saravanos[1]

[1] Department of Mechanical Engineering and Aeronautics, University of Patras,
26504 Rio-Patras, Greece
d.dimitriou@upnet.gr, c.nastos@tudelft.nl,
dsaravanos@upatras.gr

[2] Structural Integrity and Composites Group, Aerospace Engineering Faculty,
Delft University of Technology, Kluyverweg 1, Delft 2629 HS, The Netherlands

Abstract. A multiresolution finite wavelet domain method, that utilizes Daubechies wavelet and scaling functions for the hierarchical approximation of state variables, is presented. The multiresolution approximation yields a hierarchical set of equations of motion involving the coarse component of generalized displacements, while additional equations of finer components are subsequently added. A coarse solution is first calculated, and finer solutions can be sequentially superimposed on the coarse solution until convergence to the final solution is achieved. Moreover, it is shown that each resolution can model specific bandwidths of wavenumbers, thus providing a unique capability to separate coexisting wave modes and detect converted and reflected waves in the presence of damage. Two wavelet-based beam elements are explored, the first encompasses the Timoshenko shear beam theory and the second a high-order layerwise laminate theory for the accurate prediction of both symmetric and antisymmetric guided waves. Numerical results illustrate the inherent property of the method to a priori localize and isolate coexisting guided wave modes and their conversions, induced by different material regions and weak or debonded layer interfaces, thus demonstrating the method's intrinsic capabilities towards the design of wave-based SHM systems.

Keywords: Multiresolution analysis · Guided waves · Composite beams · Damage detection · Daubechies wavelets · Transient analysis

1 Introduction

During the last decades, the transient dynamic response of composite structures is intensively explored in Structural Health Monitoring (SHM) applications. In particular, guided wave-based SHM is intensively investigated due to the relatively cheap operational cost, the capability to scan large areas and the ability to detect small

imperfections/damage [1]. The design of wave-based SHM systems requires powerful and efficient simulation techniques because of the highly transient nature of such physical problems and the complexity of the involved structures.

Traditional computational methods such as the Finite Element, Boundary Element and Finite Difference method need really dense spatial and temporal discretization for the accurate solution of such problems and do not provide any additional functionalities or links with damage identification techniques. On the other hand, wavelet-based computational methods share the same basis functions as many damage detection/feature extraction schemes [2, 3]. Various wavelets like the B-spline or Daubechies have been employed for the development of wavelet-based methods for static and dynamic simulations [4–8]. Those methods employ only the scaling functions of each wavelet family, so they don't take advantage of the multiresolution (MR) property that several wavelet families possess.

However, during the past few years, the implementation of the multiresolution approach in computational methods for mechanics has been reported. Wang et al. have constructed finite element multiwavelets using linear Lagrange and cubic Hermite scaling functions that showed very good results in static analyses of rods and beams [9]. Liu et al. have proposed a multiresolution wavelet Galerkin method using Daubechies wavelets for the static solution of 2D problems [10]. Theodosiou has developed a methodology to design custom, non-uniform B-Spline wavelets with orthogonal derivatives for the hierarchical solution of static problems [11]. Liu et al. have created a multiresolution interpolation Galerkin approach for targeted solution enrichment of static problems [12]. Shen et al. have utilized multiresolution B-spline wavelet on the interval (BSWI) element for the prediction of dispersion characteristics for 2D elastic waves [13].

Most of the aforementioned methods are confined to static or steady-state dynamic simulations and don't address highly transient wave propagation analyses. Also, to the best of our knowledge, none of the previous or the other well-established numerical methods have demonstrated inherent damage detection properties that can assist the effective design of SHM systems. Recently, the authors introduced the Multiresolution finite wavelet domain (MR-FWD) method for the rapid simulation of elastic wave propagation in rods, 2D plane strain solids [14] and Timoshenko beams [15]. The MR-FWD method exhibits critical computational gains by exploiting the non-converged solution to achieve convergence and evinces extra functionalities such as the ability to leave the mesh practically unchanged when increasing the order of interpolation (p-method) because of its meshless character.

In this work, the MR-FWD method is expanded with the incorporation of a high order layerwise laminate theory [16, 17] for the accurate prediction of higher symmetric and antisymmetric guided wave modes, even at thick composites such as sandwich configurations. Additionally, the performance and enhanced capabilities of the MR-FWD method are showcased and quantified in the simulation of symmetric and antisymmetric guided waves in laminated composite beams. The numerical results are focused on the inherent localization and isolation properties of the method.

2 Theoretical Background

2.1 Daubechies Wavelets and the Multiresolution Approximation

The Daubechies (DB) wavelet family consists of compactly supported orthogonal scaling functions (SFs) $\varphi(x)$ and wavelet functions (WFs) $\psi(x)$. Both SFs and WFs are required to form the multiresolution approximation [18]. Their basic mathematical properties are outlined:

Compact Support. Both SFs and WFs are bounded within an interval, which spans over a compact support domain of grid points [0, 2 L − 1], where L is the order of the SF/WF. For the sake of conciseness, DB WFs/SFs of order L are termed as DBL. In Fig. 1 the DB8 SFs/WFs and their frequency content are shown.

Orthogonality. The integer translates of the SFs/WFs are orthogonal to each other, so they form an orthogonal basis in the Lebesgue space.

$$\int_{-\infty}^{\infty} \varphi(x-i)\varphi(x-j)dx = \delta_{ij}, \int_{-\infty}^{\infty} \psi(x-i)\psi(x-j)dx$$
$$= \delta_{ij}, \int_{-\infty}^{\infty} \varphi(x-i)\psi(x-j) = 0 \tag{1}$$

Vanishing Moments. The number of vanishing moments indicates the degree of polynomial that can be exactly approximated by SF/WF. DB SFs/WFs of order L have L vanishing moments and can exactly represent polynomials up to L-1 order.

Two Scale Relation/Dilation Property. The dilation property constitutes the basis for the MR analysis. It is provided by the dilation equations,

$$\varphi(2^j x) = \sqrt{2} \cdot \sum_{k=0}^{2L-1} h_k \cdot \varphi(2^{j+1}x - k), \psi(2^j x) = \sqrt{2} \sum_{k=0}^{2L-1} (-1)^k h_{2L-k-1} \cdot \varphi(2^{j+1}x - k) \tag{2}$$

where h_k is the set of 2 L filter coefficients, and j is the resolution or scale.
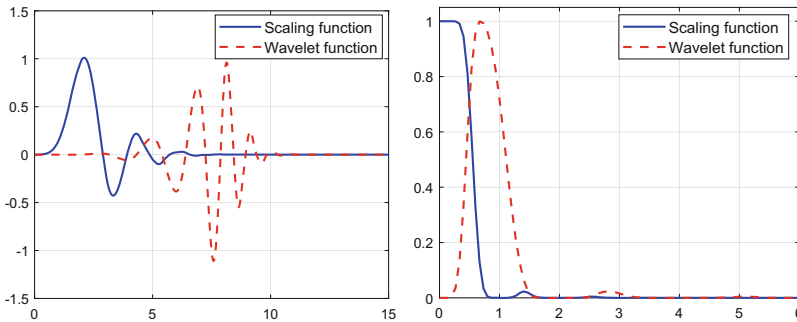

Fig. 1. Example of Daubechies SFs/WFs of order L = 8, DB8 (left), and their respective frequency content using Fourier transform (right)

2.2   The Multiresolution Finite Wavelet Domain Method

In this subsection, the generalized approximation of state variables and the formulation of the MR-FWD are briefly described. The one-dimensional MR reconstruction approach can be visualized in Fig. 2.
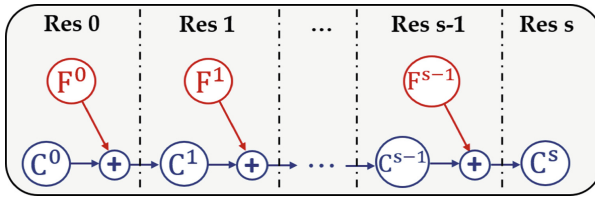

Fig. 2. Schematic diagram of the MR reconstruction procedure

In Fig. 3, a beam structure that is divided into 2 segments using a uniform grid of 3 nodes is depicted. Additional 2 L-2 grid points are introduced to the left side of the physical domain, forming the wavelet domain. The generalized displacement approximation in the segment between 2 grid points, for R resolutions is expressed as:

$$u_L(x,t) = \sum_{n=-(2L-2)}^{0} \hat{u}_{Cn}^0(t)\varphi(\xi - n) + \sum_{n=-(2L-2)}^{0} \{\sum_{S=0}^{R} \hat{u}_{Fn}^S(t)\psi(2^s\xi - n)\} \quad (3)$$

where $\hat{u}_{Cn}^0$ are the coarse wavelet coefficients at resolution 0, $\hat{u}_{Fn}^S$ are the fine wavelet coefficients at resolution S. The support domain of the MR approximation of the field variables in Eq. (3) is not confined in a finite volume or element, therefore, it yields a meshless method. For the shake of brevity, the term "element" is used to describe the segment between 2 grid points. A normalized local coordinate system ξ, is associated with each element (Fig. 3). In Fig. 2 it is shown that the MR procedure starts with the coarse solution (C^0), and then that solution is incrementally enriched by the fine solutions of each resolution (F^i).
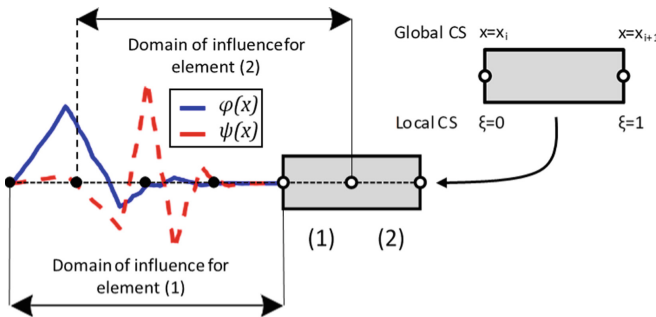

Fig. 3. Discretization of the wavelet domain for two DB3 MR wavelet-based elements

Single-Resolution or Resolution 0 (C^0). The C^0 solution is obtained employing only the DB SFs and is the same as the FWD method. The equation of motion is:

$$[M_{CC}]\ddot{\hat{u}}_{CC}(t) + [K_{CC}]\hat{u}_{CC}(t) = F_C(t) \tag{4}$$

where $\hat{u}_{CC}$ are the generalized wavelet coefficients that correspond to the degrees of freedom of the coarse approximation, $[K_{CC}]$ and $[M_{CC}]$ are the coarse resolution stiffness and mass matrices, and F_C is the coarse resolution load vector.

Resolution 1 (C^1). According to the MR process, the fine solution at resolution 0 (F^0) needs to be calculated and added to the coarse solution at resolution 0 (C^0) so as to obtain C^1 solution. The MR solution system is:

$$\begin{bmatrix} M_{CC} & 0 \\ 0 & M_{FF} \end{bmatrix} \begin{Bmatrix} \ddot{\hat{u}}_C(t) \\ \ddot{\hat{u}}_F(t) \end{Bmatrix} + \begin{bmatrix} K_{CC} & K_{CF} \\ K_{FC} & K_{FF} \end{bmatrix} \begin{Bmatrix} \hat{u}_C(t) \\ \hat{u}_F(t) \end{Bmatrix} = \begin{bmatrix} F_C(t) \\ F_F(t) \end{bmatrix} \tag{5}$$

where $\hat{u}_F$ are the generalized fine wavelet coefficients, $\hat{u}_C$ are the generalized coarse wavelet coefficients of the coupled equations of motion for resolution 1, $[K_{FF}]$ and $[M_{FF}]$ are the fine resolution stiffness and mass matrices, respectively, and F_F is the fine resolution load vector. It should be noted that $\hat{u}_C$ is not equal to $\hat{u}_{CC}$ because of the stiffness coupling terms, $[K_{CF}]$ and $[K_{FC}]$. On the other hand, $[M_{CF}]$ and $[M_{FC}]$ are equal to zero because of the cross-orthogonality between SFs and WFs, so the total mass matrix is resolution-decoupled. Moreover, due to the orthogonality of SFs and WFs, $[M_{CC}]$ and $[M_{FF}]$ are diagonal and consistent.

The hierarchical MR approach is a two-step process. First, the C^0 solution (single resolution) is obtained. Then, to take advantage of the already calculated C^0 solution, the component $\hat{u}_C$ at resolution 1 (Eq. 5) is set as $\hat{u}_C = \Delta\hat{u} + \hat{u}_{CC}$. The $\Delta\hat{u}$ is the residual between $\hat{u}_C$ and $\hat{u}_{CC}$. So, Eq. 5 can be expressed as:

$$\begin{bmatrix} M_{CC} & 0 \\ 0 & M_{FF} \end{bmatrix} \begin{Bmatrix} \Delta\ddot{\hat{u}}(t) \\ \ddot{\hat{u}}_F(t) \end{Bmatrix} + \begin{bmatrix} K_{CC} & K_{CF} \\ K_{FC} & K_{FF} \end{bmatrix} \begin{Bmatrix} \Delta\hat{u}(t) \\ \hat{u}_F(t) \end{Bmatrix} = \begin{bmatrix} 0 \\ F_F(t) - K_{FC}\hat{u}_{CC}(t) \end{bmatrix} \tag{6}$$

Employing central differences explicit integration, the diagonality of the total mass matrix results in two uncoupled equations for the prediction of $\Delta\hat{u}$ and $\hat{u}_F$. The total resolution 1 solution (C^1) is given as $\hat{u}^1_{CC} = \hat{u}^0_{CC} + \Delta\hat{u}^0 + \hat{u}^0_F$. For the interested reader, the hierarchical MR process for resolution S is meticulously described in [14, 15].

2.3 High-order Layerwise Laminate Theory

A High-order Laminate Layerwise Theory (HLLT) is encapsulated in the MR-FWD method. The kinematic assumptions of the HLLT [16, 17] are expressed as:

$$\begin{aligned} u(x,z,t) &= u^1(x,t)\Psi^1(\zeta) + u^2(x,t)\Psi^2(\zeta) + \gamma_x(x,t)\Psi^3(\zeta) + \delta_x(x,t)\Psi^4(\zeta) \\ w(x,z,t) &= w^1(x,t)\Psi^1(\zeta) + w^2(x,t)\Psi^2(\zeta) + \gamma_z(x,t)\Psi^3(\zeta) + \delta_z(x,t)\Psi^4(\zeta) \end{aligned} \tag{7}$$

where superscript $i = 1, 2$ denotes the bottom and top surface of a discrete layer with regards to the axial displacements (u) and vertical displacements (w), γ and δ are hyper-rotations, and the interpolation functions $\Psi(\zeta)$ are given as $\Psi^1 = (1 - \zeta)/2$, $\Psi^2 = (1 + \zeta)/2$, $\Psi^3 = -(\zeta^2 - 1)/2$ and $\Psi^4 = -\zeta(\zeta^2 - 1)/6$ in which $\zeta = 2z/h$ is the non-dimensional thickness variable.

3   Numerical Results

3.1   Composite Beam with First-order Shear Kinematic Assumptions

The localization and isolation capabilities of the MR-FWD method are initially demonstrated in the simulation of guided waves in a damaged laminated beam modeled with Timoshenko wavelet-based beam elements. The formulation of the wavelet-based Timoshenko beam elements is described in [15]. The laminated beam is 1 m long, with a lay-up of $[0/90/0/90]_S$ carbon/epoxy plies, has a cross section of 10^{-4} m^2, is clamped at its left edge and transversely excited at its center by a 5-cycle tone burst with 50 kHz central frequency. The damage is assumed to induce 80% degradation to all the elastic moduli. The damaged area ranges from 0.5714 m < x < 0.6714 m. The mechanical properties of the involved materials are shown in Table 1.

Table 1.   Mechanical properties of the carbon/epoxy plies

E_{11} (GPa)	$E_{22} = E_{33}$ (GPa)	$G_{12} = G_{23} = G_{13}$ (GPa)	$v_{12} = v_{13} = v_{23}$	ρ (kg/m^3)
120	7.9	5.5	0.3	1580

The MR analysis starts with the SR approximation (C^0) that involves 70 DB8 elements. The vertical displacement field of each component is shown in spatiotemporal surface plots (Fig. 4). Those plots depict the evolution of the wave propagation phenomenon both in space and time. It is captivating to observe that the C^0 solution (w_{CC}^0) does not enter the damaged region because of the higher wavenumber content inside the damage (Fig. 4a). The reflection at the damage interface is clear, and it seems that there is no transmitted wave inside the damage or beyond it. However, the residual term Δw^0 can predict the wave packet inside the healthy region at the right side of the damage (x > 0.6714 m) but does not participate in the solution inside the damage (Fig. 4b). The residual term mainly rectifies the erroneously dispersive coarse solution. The wave packet in the damage span is isolated by the fine component w_F^0(Fig. 4c). In that way, the participation of the w_{CC}^0 and Δw^0 solution at the resolution 1 solution (w_{CC}^1 or C^I) are confined in the healthy region, whereas the solution inside the damage has essentially emanated from the w_F^0 solution (Fig. 4d). The performance of the coarse and fine solutions originates from the low-pass filter behavior of the DB SFs and the band-pass filter behavior of the DB WFs (Fig. 1).
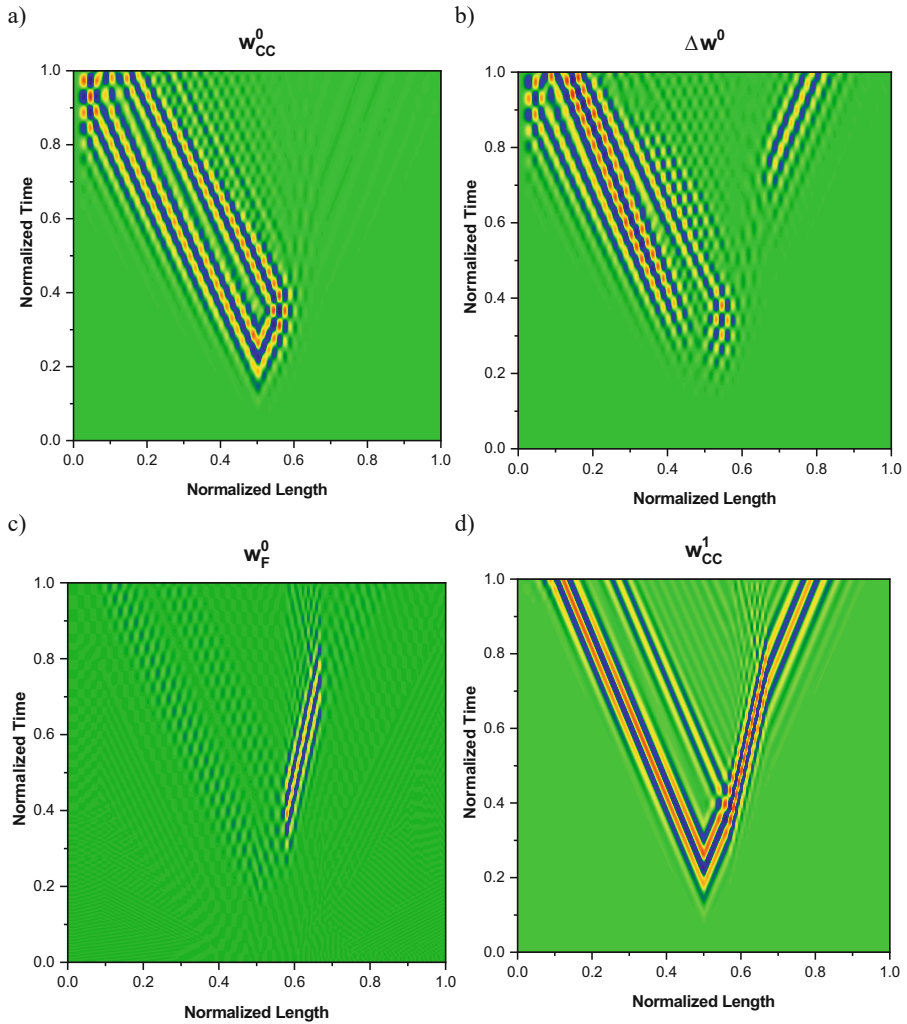
a) w_{CC}^0

b) Δw^0

c) w_F^0

d) w_{CC}^1

Fig. 4. Predicted transverse displacement field for each component till resolution 1: a) coarse component, b) residual component, c) fine component, d) total C^1 solution

3.2 Composite Beam Using HLLT

The MR-FWD method is extended with the incorporation of high-order layerwise expansion, enabling the efficient simulation of both symmetric and antisymmetric wave modes, the enforcement of surface shear excitation and the modelling of partially embedded delaminations (PED) [19]. A guided wave propagation case in a delaminated composite beam modelled with HHLT is showcased. The unidirectional laminated strip is 0.4 m long, with total thickness of 1 mm and width of 20 mm. It is clamped at its left edge and transversely excited at its top and bottom face at x = 0.2 m by a 5-cycle tone burst with 200 kHz central frequency, so as to generate an A_0 wave. The delamination

is modelled as a PED, namely a discrete layer with 0.1 mm thickness and material properties that are degraded to the 1% of the pristine carbon/epoxy (Table 1). The delaminated area ranges from 0.24 m < x < 0.4 m, as shown in Fig. 5 with the dark grey.
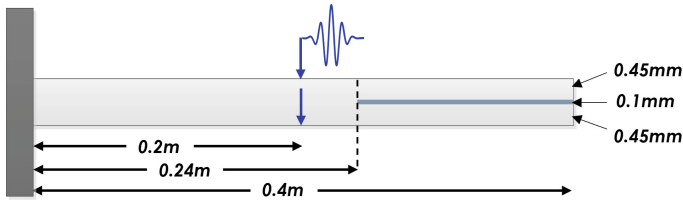

Fig. 5. Geometrical representation of the delaminated composite strip

The composite beam is modelled with three discrete layers, so as to fully represent the independent motion of the top and bottom sublaminate in the delaminated region. The MR analysis involves 260 DB6 elements and goes up to resolution 1. The axial and vertical displacement field of the top face of the beam structure are illustrated in Fig. 6 for resolution 1 solution (C^I). In view of the vertical displacement (W), the delamination can be perceptible by the reflected A_0 wave packet. When it comes to the axial displacement (U), it is obvious that an S_0 wave is generated after the incident A_0 wave enters the delaminated region. The S_0 wave exhibits a smaller wavenumber.
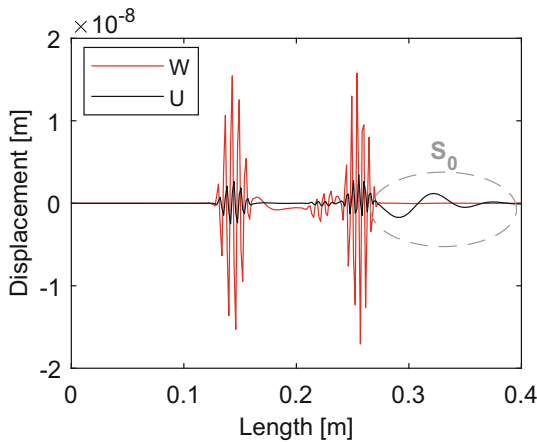

Fig. 6. Axial (U) and vertical (W) displacement field of the top surface of the composite beam at t = 0.05 ms (C^I solution)

The axial strains at the top and bottom surface of the beam are shown in Fig. 7. It is observed that the fine solution (Fig. 7 Right) isolates the A_0 wave packets due to its higher wavenumber and does not capture the S_0 wave at all, because of the already

mentioned filter-like behavior of the DB SFs/WFs. That can result to additional detection features even if the time series from a single sensor are used.

In Fig. 8, the axial strain of the top and bottom surface is presented at x = 0.26 m. The noted difference between the total (C^1) and fine (F^0) solution signal (Fig. 8 Left) indicates the presence of the S_0 wave and can be used to extract the time of flight of the S_0 and A_0 wave. Therefore, the proposed method provides a baseline-free detection feature that emanates from the multiple resolution components of the total solution.
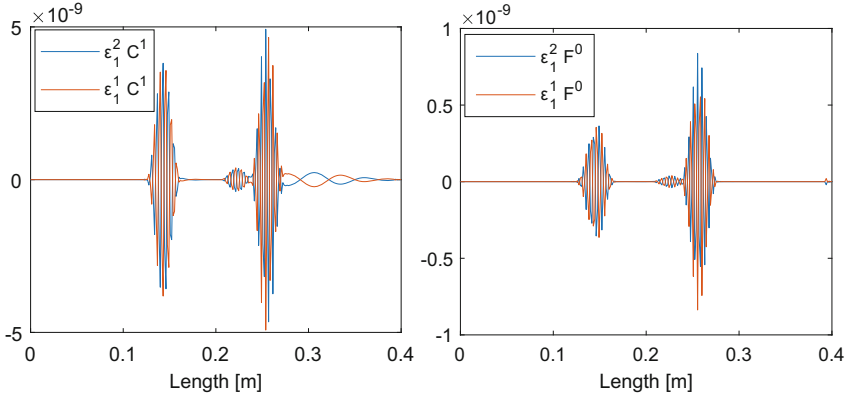

Fig. 7. Axial strain fields of the top (superscript: 2) and bottom (superscript: 1) surface of the beam at t = 0.05 ms. Left: C^1 solution. Right: F^0 solution
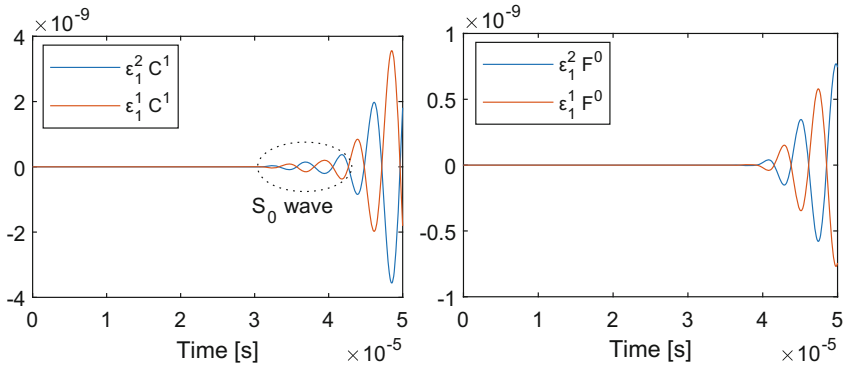

Fig. 8. Axial strain of the top (superscript: 2) and bottom (superscript: 1) surface of the beam at x = 0.26 m. Left: C^1 solution. Right: F^0 solution

4   Conclusions

In this work, the localization and isolation capabilities of the MR-FWD method are demonstrated in the simulation of guided wave propagation in damaged composite beams. The MR-FWD method is expanded with the inclusion of a high-order laminate

layerwise theory for the though-thickness approximation that permits the efficient modelling of symmetric and antisymmetric guided waves and partially embedded delaminations. The presented case studies manifest the remarkable detection capabilities of the proposed method both in spatial and temporal domain. Consequently, either with full-field measurements or with point sensors, the proposed method is able to provide additional damage detection information. Future work may focus on the processing of experimental data for the exploitation of the enhanced capabilities of the MR-FWD method in the design of SHM systems.

References

1. Ostachowicz, W., Kudela, P., Krawczuk, M., Zak, A.: Guided Waves in Structures for SHM (2012)
2. Chui, C.: An Introduction to Wavelets. Academic Press, San Diego, CA (1992)
3. Su, Z., Ye, L.: Identification of Damage Using Lamb Waves: From Fundamentals to Applications. Springer, London (2009)
4. Xiang, J.W., Chen, X.F., He, Z.J., Dong, H.B.: The construction of 1D wavelet finite elements for structural analysis. Comput. Mech. **40**, 325–339 (2007). https://doi.org/10.1007/s00466-006-0102-5
5. Zuo, H., et al.: Analysis of laminated composite plates using wavelet finite element method and higher-order plate theory. Compos. Struct. **131**, 248–258 (2015). https://doi.org/10.1016/j.compstruct.2015.04.064
6. Nastos, C.V., Theodosiou, T.C., Rekatsinas, C.S., Saravanos, D.A.: A finite wavelet domain method for the rapid analysis of transient dynamic response in rods and beams. C - Comput.. Model. Eng. Sci. **107**, 379–409 (2015). https://doi.org/10.3970/cmes.2015.107.379
7. Nastos, C.V., Theodosiou, T.C., Rekatsinas, C.S., Saravanos, D.A.: A 2D Daubechies finite wavelet domain method for transient wave response analysis in shear deformable laminated composite plates. Comput. Mech. **62**, 1187–1198 (2018). https://doi.org/10.1007/s00466-018-1558-9
8. Nastos, C.V., Saravanos, D.A.: A finite wavelet domain method for wave propagation analysis in thick laminated composite and sandwich plates. Wave Motion **95**, 102543 (2020). https://doi.org/10.1016/j.wavemoti.2020.102543
9. Wang, Y., Chen, X., He, Y., He, Z.: The construction of finite element multiwavelets for adaptive structural analysis. Int. J. Numer. Meth. Biomed. Eng. **27**(4), 562–584 (2011). https://doi.org/10.1002/cnm.1320
10. Liu, Y., Liu, Y., Cen, Z.: Multi-scale Daubechies wavelet-based method for 2-D elastic problems. Finite Elem. Anal. Des. **47**, 334–341 (2011). https://doi.org/10.1016/j.finel.2010.11.004
11. Theodosiou, T.C.: Derivative-orthogonal non-uniform B-Spline wavelets. Math. Comput. Simul. **188**, 368–388 (2021). https://doi.org/10.1016/j.matcom.2021.04.012
12. Liu, X., Liu, G.R., Wang, J., Zhou, Y.: A wavelet multiresolution interpolation Galerkin method for targeted local solution enrichment. Comput. Mech. **64**, 989–1016 (2019). https://doi.org/10.1007/s00466-019-01691-6
13. Shen, W., Li, D., Ou, J.: Dispersion analysis of Multiscale wavelet finite element for 2D elastic wave propagation. J. Eng. Mech. **146**, 1–17 (2020). https://doi.org/10.1061/(ASCE)EM.1943-7889.0001756

14. Nastos, C.V., Saravanos, D.A.: Multiresolution Daubechies finite wavelet domain method for transient dynamic wave analysis in elastic solids. Int. J. Numer. Methods Eng. **122**, 7078–7100 (2021). https://doi.org/10.1002/nme.6822

15. Dimitriou, D.K., Nastos, C.V., Saravanos, D.A.: Multi-resolution finite wavelet domain method for fast transient dynamic analysis in homogeneous and heterogeneous rods and beams. In: 8th International Conference on Computational Methods in Structural Dynamics and Earthquake Engineering, pp. 1458–1475 (2021). https://doi.org/10.7712/120121.8573.19594

16. Plagianakos, T.S., Saravanos, D.A.: Higher-order layerwise laminate theory for the prediction of interlaminar shear stresses in thick composite and sandwich composite plates. Compos. Struct. **87**, 23–35 (2009). https://doi.org/10.1016/j.compstruct.2007.12.002

17. Rekatsinas, C.S., Nastos, C.V., Theodosiou, T.C., Saravanos, D.A.: A time-domain high-order spectral finite element for the simulation of symmetric and anti-symmetric guided waves in laminated composite strips. Wave Motion **53**, 1–19 (2015). https://doi.org/10.1016/j.wavemoti.2014.11.001

18. Daubechies, I.: Ten Lectures on Wavelets. SIAM (1992)

19. Siorikis, D.K., Rekatsinas, C.S., Chrysochoidis, N.A., Saravanos, D.A.: A cubic spline layerwise spectral finite element for robust stress predictions in laminated composite and sandwich strips. Eur. J. Mech. A/Solids **91**, 104362 (2022). https://doi.org/10.1016/j.euromechsol.2021.104362